Molecular design of light-responsive hydrogels, for in-situ generation of fast and reversible valves for microfluidic applications

Jeroen ter Schiphorst,[†,#] Simon Coleman,[‡,#] Jelle E. Stumpel,[†] Aymen Ben Azouz,[‡] Dermot Diamond[*,‡] and Albertus P.H.J. Schenning[*,†,§]

†Functional Organic Materials and Devices, Department of Chemical Engineering and Chemistry, and

§Institute for Complex Molecular Systems, Eindhoven University of Technology, P.O. Box 513, 5600 MB, Eindhoven, The Netherlands

‡ INSIGHT Centre for Data Analytics, National Center of Sensor Research, Dublin City University, Dublin 9, Ireland.

ABSTRACT: Light-responsive hydrogel valves with enhanced response characteristics compatible with microfluidics have been obtained by optimization of molecular design of spiropyran photoswitches and gel composition. Self-protonating gel formulations were exploited, wherein acrylic acid was copolymerized in the hydrogel network as an internal proton donor, to achieve a swollen state of the hydrogel in water at neutral pH. Light-responsive properties were endowed upon the hydrogels by copolymerization of spiropyran chromophores, using electron withdrawing and donating groups to tune the gel-swelling rate. Faster macroscopic swelling of the hydrogels was obtained by changing an ester to an ether at the 6' position (factor of 4) or shifting the ether group to the 8' position of the spiropyran (factor of 2.5) producing a 10 fold increase in total. The effect was also visible in the swelling behavior of the corresponding hydrogel valves, where the observed macroscopic changes were reversible and reproducible and in agreement with the molecular kinetics. Gel-valves integrated within microfluidic channels have been fabricated and allow reversible and repeatable operation, with opening of the valve effected in 1 minute, while closing takes around 5.5 minutes.

INTRODUCTION

Light-responsive coatings and materials have been an attractive field of research in recent years.[1–5] Photo-switching allows alteration in the dimensional and structural composition of the material with highly precise and localised actuation, without direct contact between the material and the actuating stimulus and with minimum impact on environmental conditions.[6–11] This approach is appealing for optical data storage,[12] actuators[1] and valves in microfluidics.[13–21] In particular, the latter application ideally requires fast and large actuation of the valve structure in order to work efficiently. However, up to now, most examples are based on temperature responsive systems, which is not readily implementable in microfluidics. Key requirements for successful adoption are manufacturability combined with reliability, durability and low cost, particularly when employing these fluidic systems in analytical instruments at remote locations. Hydrogel based materials in which a photochrome is covalently incorporated in the polymer backbone can exhibit significant volume changes using light as the actuation stimulus.[22] Various photochromes have been studied that exhibit light-induced isomerization e.g. azobenzenes[23,24] and spiropyrans (Sp).[1] Azobenzenes isomerize from their trans to cis conformation with an accompanying relatively small change of dipole moment and molecular dimensions. However, in principle, significantly larger changes in dimensionality of a gel can be achieved using Sp-derivatives. Upon ring-opening and protonation in an acidic environment, the stable hydrophilic isomer merocyanine-H$^+$ (McH$^+$) is formed, which can trigger a macroscopic change in the overall character of a hydrogel e.g. from predominantly hydrophilic to predominantly hydrophobic, allowing repeatable swelling and shrinkage of the material, due to accompanying water uptake and release (Figure 1). By incorporating a Sp-based derivative into the backbone of this network, the hydrogel character may be switched using light, as Sp undergoes isomerization from the ring-closed hydrophobic form to the ring-opened hydrophilic form. Hydrogels have previously been investigated for valving applications in microfluidic devices[15,25] and recently, several approaches involving light-responsive poly(N-isopropylacrylamide) (pNIPAM)-based hydrogels containing a photochromic compound, that isomerizes and therefore contracts and swells the gels, have been reported. Fast opening of gel-based valve structures to allow flow has been demonstrated.[6]

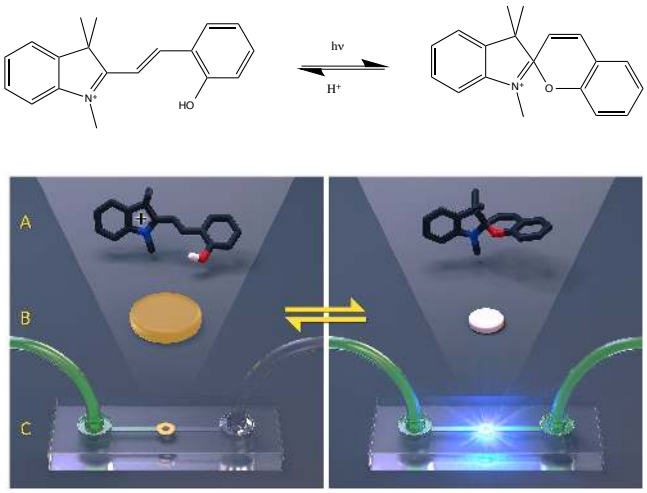

Figure 1. Isomerization of a protonated merocyanine (McH^+) and the spiropyran (Sp) form with the corresponding effect on the size of a hydrogel by irradiation with white light.

However, the time required to close these structures by re-swelling was found to be in the order of 1 hour, thus essentially limiting the potential applications to single use devices, and valves based on these gels open quickly, but take several hours to close.[7] To act as a valve, the hydrogel requires not only fast shrinkage, but also rapid swelling to close the channel in a suitable time frame, an issue that is often not discussed for such systems. Isomerization rates of Sp-s are strongly dependent on the substituents (Figure 2) as shown by Satoh *et al.*[26,27] where they investigated the system in an acidic environment. However, an acidic environment is not always desirable, as a neutral pHs are frequently required in many analytical methods and biological assays e.g. protein analysis.[7] Therefore, inspired by the work of Ziółkowski *et al.,*[9] the following study employed a self-protonating system wherein acrylic acid is copolymerized into the hydrogel to provide an internalized source of protons. Using this approach, the photo-actuation process was performed under neutral, aqueous conditions by illumination with a low-cost light-emitting diode (LED). This configuration opens up new opportunities to integrate low-cost valving functions within microfluidic systems using compact, low-cost and low-energy irradiation sources.

In this work we show how molecular design can be used to optimise molecules with improved characteristics that manifest not only at a molecular level, but also in macroscopic structures. Since the recovery (i.e. swelling) of hydrogels often is the slowest process, electron-donating groups are exploited in this work to tune the macroscopic effect of swelling using improved molecular isomerization kinetics . This is crucial to achieve an acceptable valve function in microfluidic applications, where both fast opening and closing is required to manipulate a flow; something that is often not reported for light-responsive gels. Therefore, in this paper, a systematic study on the effect of various substituents on the photo-isomerization speed of spiropyran derivatives and the corresponding macroscopic impact on hydration and dehydration of a hydrogel incorporating these derivatives is presented. This study involved the coupling of the molecular kinetics of various Sp derivatives to the corresponding shrinking/swelling kinetics of small hydrogel disks as a model study and subsequently the incorporation of the gel with fastest actuation properties into a microfluidic chip to show the reversibility and reusability of such a system..

EXPERIMENTAL SECTION

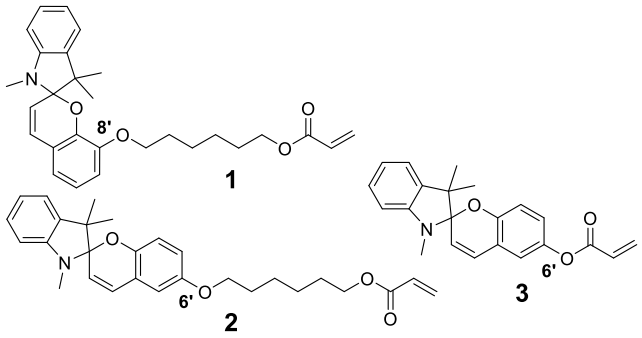

Figure 2. The synthesized structures used for this study with an ester (**3**) or ether (**2**) at the 6' position and an ether (**1**) at the 8' position.

Synthesis of the spiropyran derivative

The crude product of **1** was pre-purified by subjection to a silica column using 10% ethylacetate in heptane, before injection in a recycle GPC column using chloroform as eluents and 256 and 360 nm as detection wavelengths. ^{1}H-NMR (400 MHz, $CDCl_3$, 25°C, TMS): δ = 7.12 (t, J = 7.6, 1H, CH Ar), 7.04 (d, J = 6.3 Hz, 1H, CH Ar), 6.84 (d, J = 10.2 Hz, 1H, NCCH=CH), 6.82 – 6.76 (m, 2H, CH Ar), 6.72 (d, J = 4.9 Hz, 2H, CH Ar), 6.47 (d, J = 7.7 Hz, 1H, CH Ar), 6.41 (dd, J = 17.3, 1.4 Hz, 1H, *trans*-HC=C), 6.13 (dd, J = 17.3, 10.4 Hz, 1H, H_2C=CH), 5.82 (dd, J = 10.4, 1.4 Hz, 1H, *cis*-HC=C), 5.70 (d, J = 10.2 Hz, 1H, NCCH-CH), 4.09 (t, J = 6.7 Hz, 2H, OCH_2), 3.89 – 3.65 (m, 2H, Ar OCH_2), 2.71 (s, 3H, NCH_3), 1.58-1.43 (m, 4H, CH_2 alkane), 1.32 (s, 3H, CCH_3) 1.29-1.05 (m, 4H, CH_2 alkane), 1.18 (s, 3H, CCH_3). ^{13}C-NMR (100 MHz, $CDCl_3$, 25°C, TMS): δ = 166.32, 148.09, 146.20, 145.14, 136.92, 130.40, 129.45, 128.68, 127.33, 121.30, 120.16, 120.02, 119.58, 119.22, 118.98, 118.38, 106.62, 104.12, 70.75, 64.68, 51.37, 29.36, 28.95, 28.42, 25.74, 25.56, 25.36, 20.19. MALDI-ToF MS: m/z calcd for $C_{28}H_{33}NO_4$ $(M+H)^+$: 448.25, found: 448.29. Detailed description of the synthesis can be found in the supplementary information.

Sample preparation

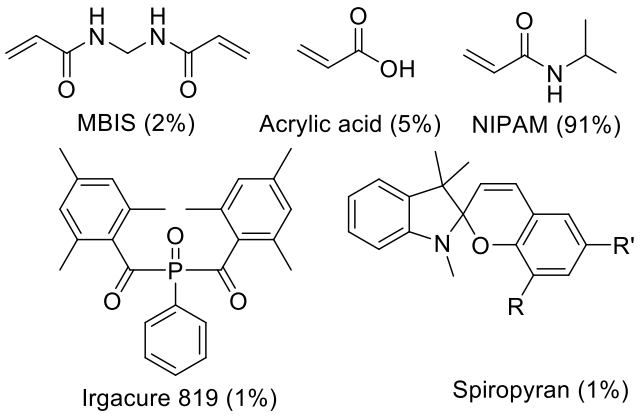

Figure 3. The materials used for preparing the light-responsive hydrogels.

Hydrogels were prepared by dissolving 91 mol% NIPAM, 5 mol% acrylic acid, 2 mol% N,N'-methylenebisacrylamide (MBIS), 1 mol% Irgacure 819 as white light photo initiator and 1 mol% of the corresponding Sp in a 2:1 mixture of dioxane and water at a ratio of 1:2 mg monomer:ml solvent (Figure 3).

To monitor the isomerization kinetics, thin films of the photoresponsive gels were prepared. Using a cell composed of two 50 micron pressure sensitive adhesive spaced glass slides filled with each monomer solution. The internal surface of the bottom slide of this cell was functionalized with 3-(trimethoxysilyl)propyl methacrylate to ensure covalent attachment of the gel to maintain a flat film for spectrometer mounting. For easy removal of the top glass slide of the cell, the corresponding glass plate is functionalized with a fluorinated compound (1H,1H,2H,2H-Perfluorodecyltriethoxysilane). Subsequently the filled cell was illuminated with white light for 15 seconds to achieve a cross-linked network. The fluorinated glass was removed and the samples were allowed to dry before being submerged in water overnight to ensure a fully equilibrated hydrated state and to remove any non-reacted monomer.

To investigate the macroscopic effects, hydrogel disks were prepared using a cell consisting of a non-functionalized microscope glass slide a 192 micron thick pressure sensitive adhesive spacer. capped with a microscope cover glass with an attached mask with 1 mm diameter holes. The material was illuminated for 15 seconds using a LED lamp at 1 cm above the mask to form the disks. The ccapping slide/mask was then removed and the valves carfully rinsed and transferred into a container filled with distilled water and left overnight to swell to ensure an equilibrium hydrated state is reached. It is assumed that the isomerization kinetics in the covalently attached material is similar to the isomerization kinetics in the hydrogel disks

Microcluidic Valve preparation and actuation

Valves were polymerized in-situ within microfluidic channels situated within PMMA chips. The two-layer chips were prepared from PMMA sheets 1.5 mm thick. The microfluidic microchannels, liquid inlet and an outlet, and a circular feature with central pillar (for housing the valve) were micromilled,on the base layer and then sealed to the top capping layer using a UV-thermal technique.. The microchannel dimensions were 1 mm wide and 0.150 mm deep, while the circular feature and pillar were 2.6 mm and 1 mm in diameter, respectively. The microchannel was filled initially with the monomer solution and the valve was created by irradiation of the solution with blue LED light at 450 nm wavelength, using a suitable mask to define the valve dimensions. After creation of the valve structure in-situ, the microfluidic system was rinsed using deionized water to remove any unpolymerised material. An in-house developed LED system was subsequently used for actuation of the valves. The channels are filled with water overnight to allow the valves to fully swell and prime the chip.

Valve performance was assessed using an in-house designed constant head platform to generate a constant flow through the system. Valve opening was achieved via exposure to blue LED light for one minute, while closure occurred spontaneously when the LED light source was turned off, as thermal equilibrium favours formation of the Sp isomer. Liquid flow through the chip was monitored as the valve opened and closed using a Fluigent L FRP Flow Meter and FRP Flowboard.

RESULTS AND DISCUSSION

Molecular design and synthesis of the spiropyran

Sp derivatives were synthesized with an ester or an ether moiety at the 6' (**2** and **3**) position or an ether moiety at the 8' position (**1**), whereby the ester will withdraw electron density from the system destabilizing the open (Mc) form, while, in contrast, the ether donates electron density stabilizing the open form. The Sp-based derivatives **2** and **3** were synthesized according to procedures reported earlier,[9–11] whereas the Sp-8' derivative **1** is a novel compound and is expected to have faster isomerization kinetics to the McH^+ form compared to the Sp-6' derivatives, based on similar trends observed in the work of Satoh et al.[26] A Fisher base and the corresponding salicylaldehyde are condensed to a Sp with a hydroxyl group at the desired 6' or 8' position. Subsequently, a Williamson ether synthesis of the Sp with 6-bromohexyl acrylate under Finkelstein conditions using potassium iodine and potassium carbonate in 2-butanone results in the corresponding Sp-ether derivatives. The Sp-ester derivative was achieved by reacting the Sp-6'-OH using acryloyl chloride resulting in **3** (Figure 2).

Characterization of the hydrogels

Before switching the material with light, the amount of protonated merocyanine (McH^+) in the hydrogels was determined using UV-Vis spectrophotometry at various concentrations of HCl ranging from 0.05M to 1M. At a concentration of 1M HCl, it is assumed that Sp is completely in the McH^+ form. The hydrogel covalently attached to a glass slide (Figure 4; top) was positioned inside a custom fabricated PMMA-based cuvette allowing direct contact of water with the hydrogel. To ensure that the system was at the maximum concentration of McH^+, time dependent UV-Vis spectroscopy was used at the 1M HCl concentration. It was expected that no unprotonated merocyanine (Mc) would be present as

there was a large excess of protons under these conditions and this was confirmed by examining the wavelengths characteristic of merocyanine absorbance. Subsequently, 0.2M triethylamine in water was then brought in contact with the hydrogel to produce both the Sp and Mc form, as was indicated by the appearance of an additional absorbance peak at higher wavelengths, characteristic of Mc (Figure Sx). From this experiment one can conclude that there is no evidence of unprotonated merocyanine in the UV-Vis spectra under acidic/neutral conditions, and absorbance in the visible region was only caused by the McH^+ isomer.

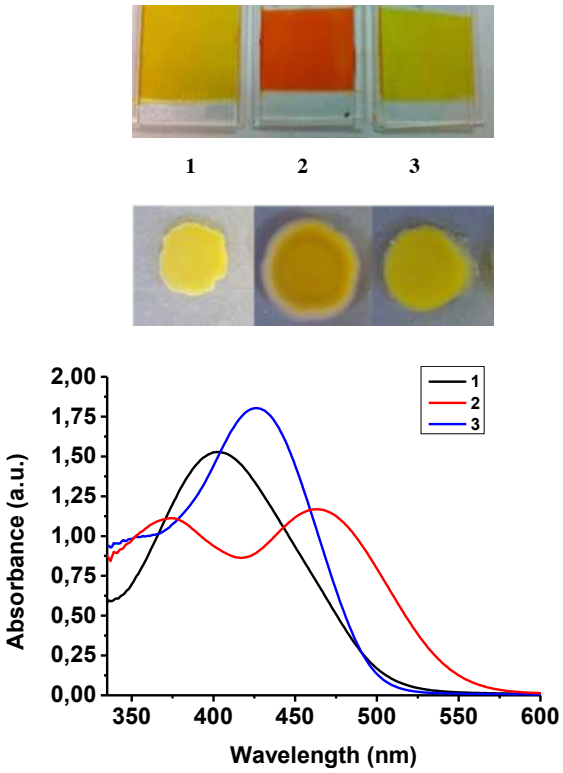

Figure 4. Top: Photographs of the surface attached hydrogels used for the kinetics measurements. Middle: Hydrogel disks made to measure the swelling effects. Bottom: UV-Vis spectra the surface attached hydrogels based on compounds **1**, **2**, **3**.

Over the spectral range studied, Compound **1** has a single strong absorbance band with a λ_{max} at 403 nm and peak absorbance of 1.53 in distilled water, which is similar that reported by Satoh et al.[26] Upon exposure to increasing concentrations of HCl, the λ_{max} shifts to ca. 430 nm and peak absorbance increases to 1.76 (1M HCl). After 150 minutes of exposure to this HCl concentration, a gradual slight increase to an absorbance of 1.82 is observed (Figure S5). Based on our previous assumptions, this suggests that around 84% of the spiropyran is in the McH^+ form (equation 2 in the supporting information). A similar procedure was used with compound **2** and **3**, resulting in 78 and 100% open form for compound **2** and **3,** respectively (Figures S6 and S7). No clear indication of presence of non-protonated merocyanine was found (vide supra).

On the macroscopic level,, the initial size of the gel disk (figure 4; middle) in deionized water was measured as the average of 3 disks (see SI). The largest disk was obtained with compound **2** (~92,850 pixels). Compound **3** had an average size of ~80,000 pixels and compound **1** an average size of ~48,850 pixels measured using ImageJ software. This is summarized in (Table 1).

Table 1. Properties of the hydrogel disks and surface attached hydrogels.

	λ_{max} (nm)	Concentration merocyanine in pure water (%)*	Initial size (pixels)***
1	403	84	48,850
2	376 467	78	92,850
3	425	100**	80,000

*Calculated using equation 2 (See SI).

** No difference found upon acidifying.

***Calculated as the average of 3 gels using the area (Figure S3)

Photoswitching and actuation of hydrogels: Shrinking the material

To measure the isomerization kinetics of McH^+ to Sp, the surface attached hydrogels in distilled water were illuminated with white light for 300 seconds before allowing the material to recover in the dark. Upon illumination, the absorbance measured at the peak maximum decreased rapidly, indicating that the isomerization of McH^+ to Sp is fast. Compound **3** requires ~12 seconds before reaching the photo-stable state (pss), while **2** and **1** require ~75 and ~90 seconds, respectively (Figure 5). This indicates that **3** has the fastest molecular closing kinetics, which is what one would expect, since the withdrawing nature of electrons of the ester stabilizes the closed Sp, while electron donating groups enhance ring opening of the molecule.

On the macroscopic level, upon exposing the equivalent gel disks to white light, rapid shrinkage of the disk occurs. During this time, a stereomicroscope was used to track the degree of shrinkage every 30 seconds, and the surface area was calculated in pixels using ImageJ (See SI). Upon plotting the area, one can see that the slope of the shrinkage is very similar in all situations, indicating that this is not dependent on the Sp derivative used. In the first run, all gel disks shrink to ca. 60% of their original area. The minimal size of the gel after 300 seconds illumination was 65, 54 and 58% of the initial area or 80, 74 and 76% of the initial radius for the hydrogels containing **1**, **2** and **3,** respectively (Figure 5). Interestingly all gels seemed to reach the same relative final size, indicating that the addition of **2** allows the gel to swell more than the other derivatives (Figure S3). No explanation was found for this phenomenon.

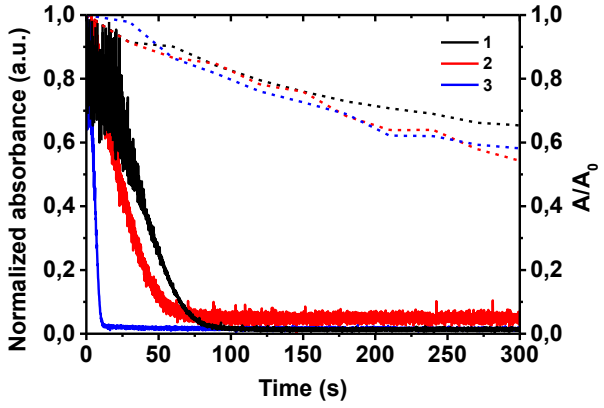

Figure 5. The isomerization of McH^+ to Sp in both the surface attached hydrogel (solid line) and the corresponding shrinkage (dashed line) of the hydrogel disks during 300 seconds irradiation with white light. The absorbance was measured at the λ_{max}; 403, 467 and 425 nm for **1**, **2** and **3**, respectively.

Photoswitching and actuation of hydrogels: Recovery of the material

When the material is allowed to reswell in the dark for 1800 seconds, the formation of McH^+ can be tracked over time using UV-Vis spectroscopy. The protonation process of Sp to McH^+ appeared to follow 1st order kinetics in all three cases. In Fig. 6, the normalized absorbance plot shows that **1** has the fastest ring opening kinetics indicated by the slope. After 1800 seconds, **1** recovered to 92% of the original protonated merocyanine absorbance, while **3** and **2** only recovered to 65% and 38% of the original absorbance, respectively. The isomerization rate coefficient $k_{Sp\rightarrow McH}$ of **1** was found to be $2{,}78x10^{-3}$ s^{-1}, while **2** is $1{,}08x10^{-3}$ s^{-1} and **3** is $2{,}77x10^{-4}$ s^{-1} making **1** ca. 2.5 times faster than **2,** and ca. 10 times faster than **3**. The disks were also allowed to reswell over the same time frame and the area measured every minute. The initial size of **2** was larger than observed in the other gels. Upon swelling, only the gel containing **1** recovered its approximate initial size (95%), while the **2** and **3** recovered only 46% and 32%, respectively. The difference in size is not expected to be problematic, as the thickness (z) for all gels is defined by the production method and is far smaller than the area (x-y plane) i.e. z<<x,y.

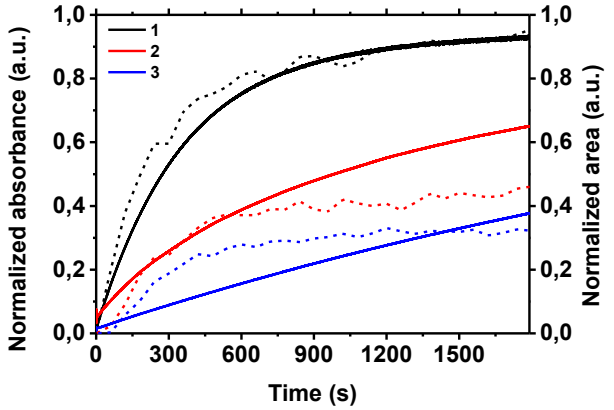

Figure 6. The isomerization of Sp to McH^+ in both the surface attached hydrogel (solid line) and the corresponding normalized area (dashed line) of the hydrogel disks during 1800 seconds in the dark. The absorbance was measured at λ_{max}; 403, 467 and 425 for **1**, **2** and **3** respectively.

This measurement was repeated three times and shows the reversibility of the McH^+ isomerization (Figure 7). The gel containing derivatives **2** and **3** decrease in size upon the second and third illumination cycle, indicating that (i) the minimal size is not reached and (ii) the swelling kinetics are slower than in the gel containing compound **1**.

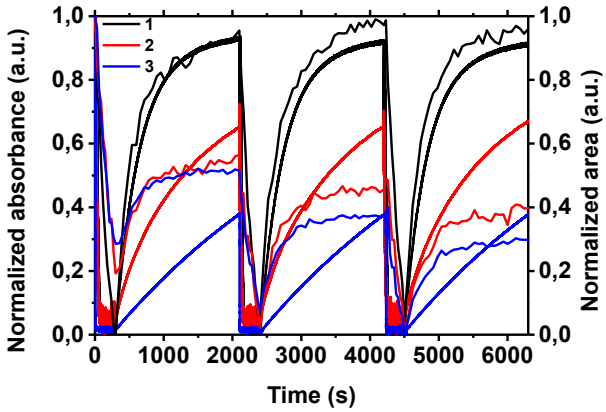

Figure 7. Normalized plot of the absorbance of the surface attached hydrogels (solid line) and the disk area (dashed line) depicting the correlation between the molecular kinetics and macroscopic swelling effects upon three consecutive illumination and relaxation runs. The absorbance was measured at λ_{max}, 403, 467 and 425 for **1**, **2** and **3**, respectively.

The hydrated gel size of derivatives **2** and **3** is observed to decrease upon multiple illuminations (Figure 7) which could potentially present a challenge when this material is used in a valve configuration, since it could potentially result in leaking through the valve. Derivative **1** exhibited the most desirable properties as its swell recovery only exhibited minor loss of original size. After three cycles of 300 seconds illuminating and 1800 seconds recovering, the size of the gel calculated by the normalized area is 96, 40 and 30% for **1**, **2** and **3** respectively. This is summarized in Table 2.

Table 2. Kinetic properties of the used hydrogel disks and surface attached hydrogels.

Gel containing spiropyran:	Photo stationary state (s)	$K_{Sp\rightarrow McH}$+ 10^3 s^{-1}	Swollen after 1800 sec (%)*
(1)	~90	2.78	96
(2)	~75	1.08	40
(3)	~12	0.277	30

*Calculated by the average of 3 gels in the last run using the normalized area.

From the results above, it was clear that **1** exhibits the greatest potential for implementation as a valve material due to its almost

complete recovery. However, derivatives **2** and **3** can also be used by optimization of their size whereby their edges are closer to the channel walls than that of **1** gels. All gel valves are optimised so that their swollen forms press against the channel walls to create a seal and the creation of a larger valve would result in over-swelling against the walls of the channel and the resulting loss during recovery will be hidden within this over-swelling component. Figure 7 implied that the loss in recovery would continue beyond 3 swell cycles and as such even with the over-swelling, the valves would be expected to fail eventually. Consequently, it appears that all three derivatives could be potentially be used as single use valves while derivative **1** shows potential for use as a permanent, reusable valve.

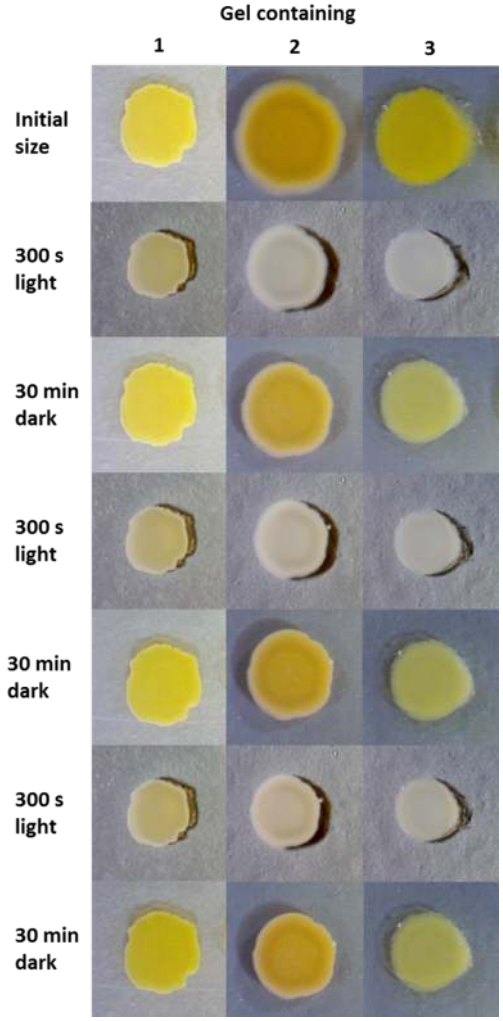

Figure 8. Photographs of the disks at the initial size and after three runs of 300 sec of illumination with white light and subsequently recovering in the dark for 1800 sec.

Isomerization kinetics versus swelling kinetics.

There are three scenarios that can occur when correlating the isomerization kinetics of the Sp derivative to the swelling and shrinking behavior of the hydrogels:

1. The kinetics of the isomerization of Sp is **faster** than the swelling or shrinking kinetics: Diffusion limitation
2. The kinetics of the isomerization of Sp is in the **same range** of the swelling or shrinking kinetics: Both processes are synchronized
3. The kinetics of the isomerization of Sp is **slower** than the swelling or shrinking kinetics: Isomerization limitation

To improve the swelling speed of the material, in the first scenario the material can be dimensionally scaled down, as there is a dependence of diffusion on the radius squared of the material. In the third scenario, improvements can be obtained by designing the molecular structure of the Sp derivative, so as to enhance the isomerization kinetics. When plotting the normalized Sp isomerization kinetics and gel swell kinetics in one plot (Figure 7), one can clearly see that the shrinking of the gel is diffusion process limited, since the pss is reached after maximal 90 seconds, while the gel does not show maximum shrinkage even after 300 seconds of illumination.

Upon reswelling, in the case of both Sp-6' derivatives (**2** and **3),** the material does not return to its original size (Figure 8). The isomerization kinetics are slower than the recovery of the material, indicating that there is an isomerization kinetics limitation. As **2** has faster Sp to McH^+ isomerization, this gel swells back to about 40% of the original size after the three illumination cycles, while **3** only recovers ca. 30% upon the third illumination cycle. **1** however exhibits full recovery its initial swollen size in the measured timespan but it is debatable whether the kinetics of isomerization for **1** are in the same range or slower than the swelling kinetics. The slope of both the swelling and isomerization curve is very similar, indicating that these two observables are directly connected to each other i.e. the hydrophilicity changes which occur upon isomerization are being translated to a change in hydrophilicity of the entire material.

When examining the swelling profile in Figure 6 and Figure 7 in more detail, two separate situations are observed for derivatives **2** and **3**. Initially, the swelling seems very steep and suddenly reaching a plateau. Therefore, an initial diffusion limitation followed by isomerization limitation is expected. This is not the case for the **1** where a gradual increase in both the kinetics and extent of swelling is observed.

Hydrogel based microvalves

Hydrogel-based valves were produced to examine the application of the macroscopic results observed above as a practical application for fluid control. Since derivative **1** exhibited the fastest isomerization kinetics and most reproducible swell/shrink profile, light-switchable valves based on this gel were created. The valve was locally illuminated using a blue LED, as can be seen in Figure 9, resulting in gel shrinkage and flow occurring in the channel a few seconds after initiation of LED illumination. After illumination for one minute, the LED was turned off and the valve allowed to spontaneously re-swell.

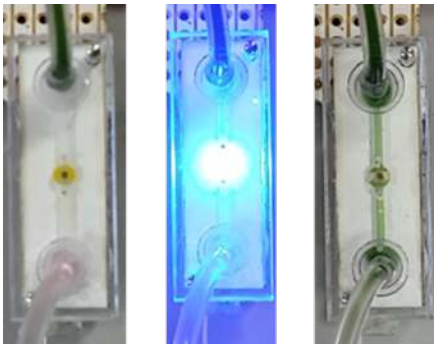

Figure 9. Valve action of a gel containing derivative **1**, polymerized in-situ within a sealed PMMA chip. Left: no flow observed with valve fully swollen and sealing channel. Centre: illumination with blue LED results in shrinking of valve. Right: open valve after 1 min illumination showing flow. The fluid passing thought the valve is colored green for visualisation. The channel was filled with clear water before attaching the tubing to ensure a swollen state of the gel.

This sequence was repeated four times (figure 10), showing that the valve actuation is reversible. To our knowledge, this is the first reported instance of such reversible behavior for this type of photo-switchable gel-valve in a microfluidic channel, and it is convincing evidence of the exciting potential of these structures to provide flexible flow control within microfluidic chips. Valve closure was essentially complete within several minutes, while opening occurred within seconds. The timescale of this on/off flow control could be further optimized, for example, by varying the LED power during the 'on' event, so that the peak flow (and therefore extent of contraction) was smaller. The smaller extent of contraction would allow correspondingly faster closure of the valve. The flow rate was found to peak at approximately 7µl/min and around 15µl volume of liquid passed during each open valve cycle.[28]

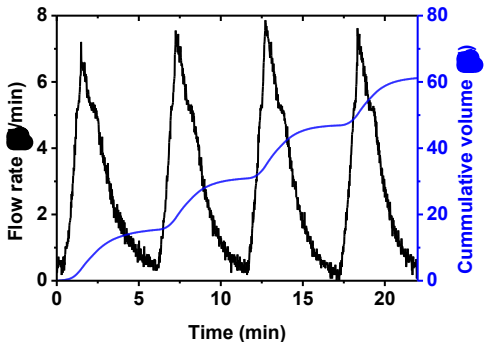

Figure 10. Flow profile of a gel with spiropyran derivative **1** upon illumination with blue light for 1 minute. A reproducible opening and closing is observed indicated by the flow profile (black) as well as the cumulative flow volume profile (blue).

CONCLUSION

This paper has demonstrated that molecular design of the photochromic compound within a hydrogel allows for direct influence upon the macroscopic level effects observed. Correctly designing of a spiropyran derivative has resulted in improvement of the reversible swelling/shrinking behavior of the hydrogels. This is not only interesting for microfluidics, but the concept can be further expanded to a large amount of actuating material applications, where design of a molecule is helpful for the macroscopic effects. Here, the concept was employed to generate a molecule that resulted in improvement of isomerization speed for a hydrogel performed in a model study. The production of efficient valving gelsIt opens up a new method of microfluidic flow control that can be widely employed in analytical devices, particularly deployable autonomous platforms, as its simplified, compact configuration and non-contact operation with LED illumination results in a low cost, low energy valve unit with functionality potentially comparable to those of existing mechanical valves.

ASSOCIATED CONTENT

Supporting Information.
Experimental methods, synthetic procedures, full characterization and optical analysis of the molecules and devices.
This material is available free of charge via the Internet at http://pubs.acs.org.

AUTHOR INFORMATION

Corresponding Author

*E-Mail: a.p.h.j.schenning@tue.nl (A.P.H.J.S.).
*E-Mail: dermot.diamond@dcu.ie (D.D)

Author Contributions

#These authors contributed equally.

Notes

The authors declare no competing financial interest.

ACKNOWLEDGEMENT

We acknowledge funding for this project under the European Union's Seventh Framework Programme for research, technological development and demonstration, through the NAPES project grant agreement no. 604241. Jeroen ter Schiphorst would like to thank Ralf Bovee and Xianwen Lou for their support with the analytical measurements. ICMS

REFERENCES

(1) Klajn, R. *Chem. Soc. Rev.* **2014**, *43* (1), 148–184.

(2) Tomatsu, I.; Peng, K.; Kros, A. *Adv. Drug Deliv. Rev.* **2011**, *63* (14-15), 1257–1266.

(3) Dai, S.; Ravi, P.; Tam, K. C. *Soft Matter* **2009**, 2513–2533.

(4) Jochum, F. D.; Theato, P. *Chem. Soc. Rev.* **2013**, *42* (17), 7468–7483.

(5) Florea, L.; Diamond, D.; Benito-lopez, F. **1952**, 15–17.

(6) Sugiura, S.; Szilágyi, A.; Sumaru, K.; Hattori, K.; Takagi, T.; Filipcsei, G.; Zrínyi, M.; Kanamori, T. *Lab Chip* **2009**, *9* (2), 196–198.

(7) Sugiura, S.; Sumaru, K.; Ohi, K.; Hiroki, K.; Takagi, T.; Kanamori, T. *Sensors Actuators A Phys.* **2007**, *140* (2), 176–184.

(8) Szilágyi, A.; Sumaru, K.; Sugiura, S.; Takagi, T.; Shinbo, T.; Zrínyi, M.; Kanamori, T. *Chem. Mater.* **2007**, *19* (11), 2730–2732.

(9) Ziółkowski, B.; Florea, L.; Theobald, J.; Benito-Lopez, F.; Diamond, D. *Soft Matter* **2013**, *9* (36), 8754.

(10) Stumpel, J. E.; Liu, D.; Broer, D. J.; Schenning, A. P. H. J. *Chemistry* **2013**, *19* (33), 10922–10927.

(11) Stumpel, J. E.; Ziółkowski, B.; Florea, L.; Diamond, D.; Broer, D. J.; Schenning, A. P. H. J. *ACS Appl. Mater. Interfaces* **2014**.

(12) Stumpel, J. E.; Broer, D. J.; Schenning, A. P. H. J. *Chem. Commun. (Camb).* **2014**.

(13) Whitesides, G. M. *Nature* **2006**, *442* (7101), 368–373.

(14) Dong, L.; Jiang, H. *Soft Matter* **2007**, *3* (10), 1223.

(15) Romero, M. R.; Arrua, R. D.; Alvarez Igarzabal, C. I.; Hilder, E. F. *Sensors Actuators B Chem.* **2013**, *188*, 176–184.

(16) Eddington, D. *Adv. Drug Deliv. Rev.* **2004**, *56* (2), 199–210.

(17) Zhang, C.; Xing, D.; Li, Y. *Biotechnol. Adv.* **2007**, *25* (5), 483–514.

(18) Arndt, K.; Kuckling, D.; Richter, A. **2000**, 505 (November 1999), 496–505.

(19) Park, S.; Kim, D.; Ko, S. Y.; Park, J.-O.; Akella, S.; Xu, B.; Zhang, Y.; Fraden, S. *Lab Chip* **2014**, No. d, 1551–1563.

(20) Kim, D.; Beebe, D. J. *Lab Chip* **2007**, *7* (2), 193–198.

(21) Moore, J. S.; Bauer, J. M.; Yu, Q.; Liu, R. H.; Devadoss, C.; Jo, B. **2000**, *404* (April).

(22) Czugala, M.; O'Connell, C.; Blin, C.; Fischer, P.; Fraser, K. J.; Benito-Lopez, F.; Diamond, D. *Sensors Actuators B Chem.* **2014**, *194*, 105–113.

(23) Russew, M.-M.; Hecht, S. *Adv. Mater.* **2010**, *22* (31), 3348–3360.

(24) Merino, E.; Ribagorda, M. *Beilstein J. Org. Chem.* **2012**, *8*, 1071–1090.

(25) Kang, D. H.; Kim, S. M.; Lee, B.; Yoon, H.; Suh, K.-Y. *Analyst* **2013**, *138* (21), 6230–6242.

(26) Satoh, T.; Sumaru, K.; Takagi, T.; Takai, K.; Kanamori, T. *Phys. Chem. Chem. Phys.* **2011**, *13* (16), 7322–7329.

(27) Satoh, T.; Sumaru, K.; Takagi, T.; Kanamori, T. *Soft Matter* **2011**, *7* (18), 8030.

(28) Footnote. .

Please note that the flow meter is operating below the calibrated value, inducing slight noice in the flows close to 0 µl/min. This has been corrected to only have positive flow, slightly overestimating the peak flow and volumes depected in Figure 10.